PRAMANA
— journal of
physics

Vol. 68, No. 4
April 2007
pp. 679–687

Synthesis and characterization of Mn^{2+}-doped ZnS nanoparticles

B S REMA DEVI, R RAVEENDRAN and A V VAIDYAN*
Crystal growth Laboratory, Department of Physics, S.N. College, Kollam 691 001, India
*Department of Chemistry, St. Stephens College, Pathanapuram, India
E-mail: remadevi1956@rediffmail.com; rrsnc@yahoo.com

MS received 11 July 2006; revised 20 December 2006; accepted 18 January 2007

Abstract. Mn^{2+}-doped ZnS nanoparticles were prepared by chemical arrested precipitation method. The samples were heated at 300, 500, 700 and 900°C. The average particle size was determined from the X-ray line broadening. Samples were characterized by XRD, FTIR and UV. The composition was verified by EDAX spectrum. The hexagonal structure of the sample was identified. The size of the particles increased as the annealing temperature was increased. The crystallite size varied from 5 nm to 34 nm as the calcination temperature increased. At around 700°C, ZnS is converted into ZnO phase due to oxidation. The emission peak of the sample is observed at 300 nm resulting in blue emission. The solid state theory based on the delocalized electron and hole within the confined volume can explain the blue-shifted optical absorption spectra. UV-VIS spectro-photometric measurement shows an indirect allowed band gap of 3.65 eV.

Keywords. Nanoparticles; nanocomposite; Mn^{2+}-doped ZnS; annealing; X-ray diffraction; FTIR; ultra violet.

PACS Nos 73.63.Bd; 61.82.Rx; 72.80.Tm; 64.70.Nd

1. Introduction

It is well-known that the optical and electronic properties change dramatically due to quantum confinement of the charge carriers within the particle [1,2]. ZnS, which is an important wide band gap semiconductor, has attracted much attention owing to its wide applications including UV light emitting diodes, efficient phosphors in flat-panel displays, photo voltaic devices etc. [3]. It is reported that ZnS doped with Mn^{2+} has a potential application in field emission devices (FED) [4]. Doped semiconductor nanoparticles $ZnS:Mn^{2+}$ is used as phosphors and also in thin film electroluminescent devices [5]. The optical properties of nanocrystalline semiconductors have been studied extensively in recent years. The band structure of the semiconductor changes with decreasing particle size. Hence, it is interesting to synthesize nanoparticles of ZnS doped with Mn^{2+} and characterize them and subject them to optical studies.

2. Experimental

Nanoparticles of Mn^{2+}-doped ZnS were prepared by chemical co-precipitation method. All the chemicals were of AR grade and were used without further purification. Freshly prepared aqueous solutions of the chemicals were used for the synthesis of nanoparticles. These particles were prepared at room temperature by dropping simultaneously 50 ml of 0.4 M solution of zinc sulphate, 50 ml of 0.1 M solution of manganese sulphate and 50 ml of 0.5 M solution of sodium sulphide into 80 ml of distilled water containing 50 ml of 0.1 M solution of EDTA which was vigorously stirred using a magnetic stirrer. The role of EDTA was to stabilize the particles against aggregation which may lead to an increase in the size of the particles. The precipitate was separated from the reaction mixture, washed several times with distilled water and then with alcohol to remove the impurities, including traces of EDTA and the original reactants, if any. The wet precipitate was dried and thoroughly ground [6].

XRD and FTIR analyses of these samples were done for their characterization. XRD patterns were recorded on a RigaKuC/max-2500 diffractometer using graphite filtered CuK_α radiation ($\lambda = 1.54056$ Å) at 40 kV and 100 mA with a scanning rate of 8° min^{-1} from $2\theta = 5^\circ$ to 80°. The XRD patterns are shown in figure 1.

The FTIR spectra were recorded in an FTIR spectrometer (Nicolet Magna-750) in the range of 500 cm^{-1} to 4000 cm $^{-1}$. The spectra were presented in figures 2a–2e.

The energy dispersive analysis of X-rays (EDAX) was done on the sample to ascertain the composition. It is presented in figure 3.

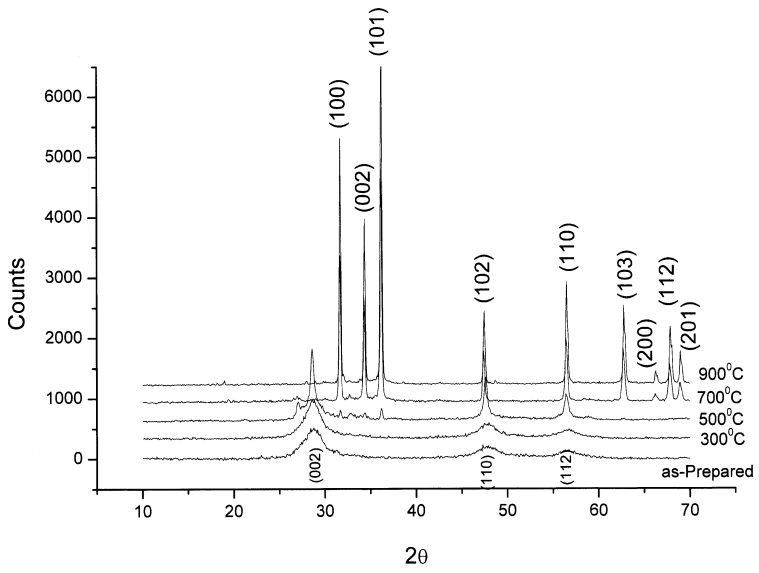

Figure 1. XRD pattern of the samples at different temperatures.

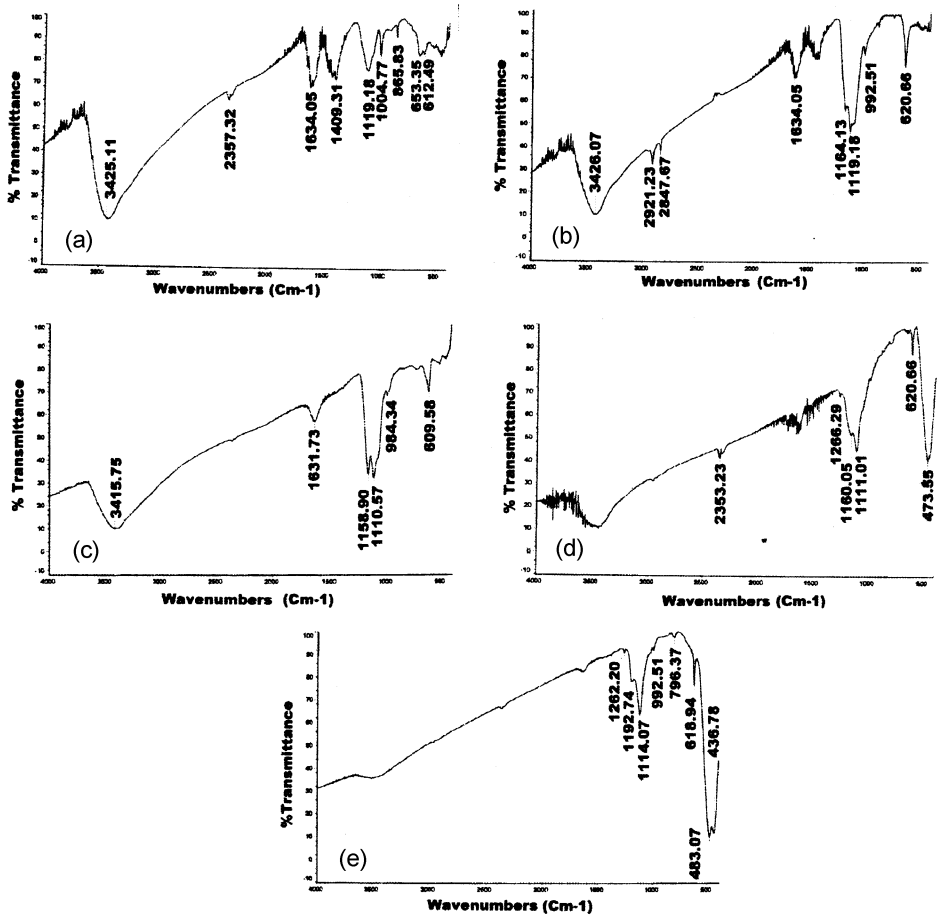

Figure 2. (**a**) FTIR at room temperature, (**b**) 300°C, (**c**) 500°C, (**d**) 700°C and (**e**) 900°C.

The UV-study of the samples was carried out with a view to explore their optical properties. The UV measurements were done with UV spectrometer JASCO V-550 in the wavelength range of 200 nm to 850 nm. The UV spectrum of the sample is

Table 1. Relation connecting temperature and grain size.

Temperature (°C)	Grain size (nm)
Room temperature	5–6
300	20
500	21–26
700	32–36
900	32–36

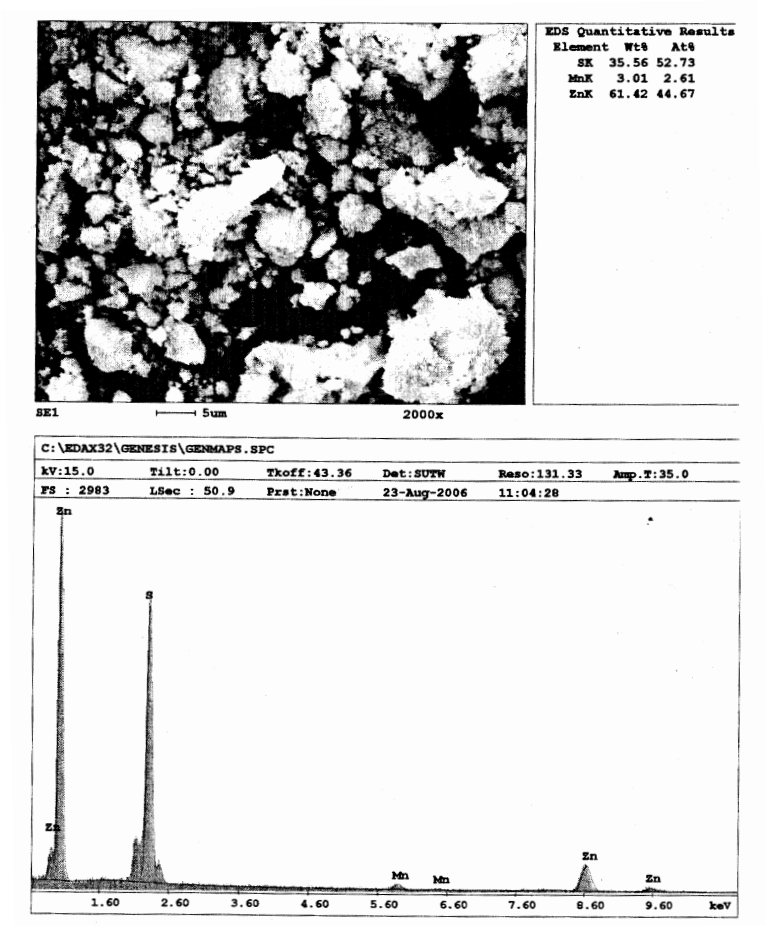

Figure 3. SEM with EDAX.

given in figure 4. The band gap calculated from the plot of $(\alpha h\nu)^2$ vs. $h\nu$ is given in figure 5.

3. Results and discussion

3.1 *XRD analysis*

Figure 1 shows the XRD patterns of the samples at different temperatures. As-prepared sample was calcined at 300, 500, 700 and 900°C for 5 h in air atmosphere to ascertain the formation of different nanocrystalline phases. Using the Debye–Scherrer formulae, the mean crystalline size was calculated from the full-width at half-maximum (FWHM) of the XRD lines. They are given in table 1. It can be

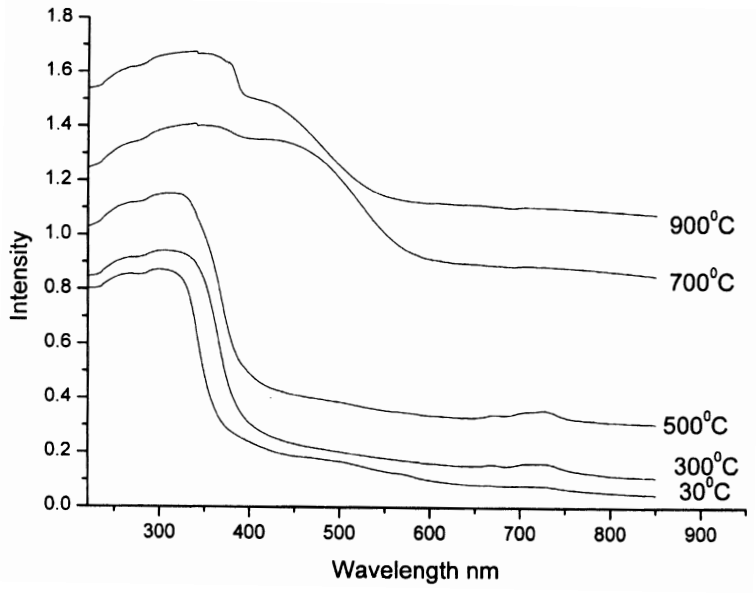

Figure 4. Intensity vs. wavelength λ. Traces of the samples.

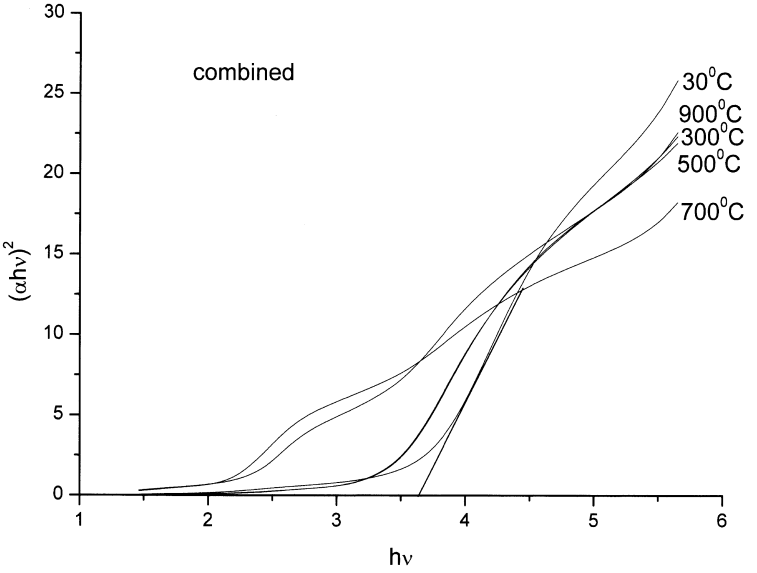

Figure 5. $h\nu$ vs. $(\alpha h\nu)^2$ of the samples.

seen that the average size of the nanoparticle increases as the heating temperature is increased. It indicates that the size of crystallites can be adjusted by controlling the annealing temperature.

Table 2. Observed and calculated X-ray diffraction data of the sample.

d (Å)	Relative intensity	2θ		$\Delta 2\theta$	$h\ k\ l$	a (Å)
		Observed	Calculated			
3.13007	100	28.501	28.493	0.008	0 0 2	6.260
1.90691	30.96	47.562	47.650	−0.088	1 1 0	2.696
1.62572	22	56.393	56.564	−0.17	1 1 2	3.982

Table 3. IR peaks and their assignments.

Wave number ($\times 10^{-2}$ m^{-1})	Assignment
3425	O–H stretching
1634	O–H bending
1164	Symmetric stretching
1119	Asymmetric stretching
1004	Shoulder with asymmetric stretching
865	Additional asymmetric stretching
612	Symmetric bending
473	Asymmetric bending

Table 4. Relation between temperature of the samples and the band gaps.

Temperature (°C)	eV
As prepared	3.7
300	3.18
500	3.0
700	2.1
900	2.1

It is seen from table 2 that ZnS nanoparticles exhibit structure of bulk ZnS in comparison (JCPDS file No. 36-1450) in which the space group P63mc(186) with the lattice constant $a = 0.3820$ nm and $c = 0.6257$ nm is indicated. In our case three peaks at diffraction angle (2θ) of 28.501°, 47.562° and 56.383° correspond to the (0 0 2), (1 1 0) and (1 1 2) lattice planes of hexagonal ZnS respectively. It is observed that after annealing at 700°C for 5 h the diffraction peaks of ZnS disappeared and ZnS phase is completely transformed into ZnO phase. All diffraction peaks in the patterns of the ZnO nanoparticles are indexed to the hexagonal wurtzite structure (JCPDS No. 36-1451). It is likely that at 700°C and above, the ZnS is completely oxidized to ZnO in atmospheric air as shown by the equation [7].

$$2\mathrm{ZnS}_{(\mathrm{S})} + 3O_{2(\mathrm{g})} = 2\mathrm{ZnO}_{(\mathrm{S})} + 2\mathrm{SO}_{2(\mathrm{g})}.$$

When annealing temperature is increased to 900°C the diffraction peaks become sharper and stronger which suggest that the crystal quality of the resultant nanoparticle is improved and the particle size is larger.

It is also observed that the sample heated up to 500°C shows light brownish white color, sample heated up to 700°C show dark brown color and rocky appearance while sample heated up to 900°C exhibit yellowish green color and highly scattered appearance. The color of the sample indicates that Mn^{2+} may be incorporated in the crystal lattice.

3.2 *FTIR studies*

In table 3, IR peaks are assigned to samples at room temperature. The samples at room temperature, heated at 300°C and 500°C show characteristic peaks at 612, 865, 1004, 1119 cm^{-1} and some other associated peaks (figures 2a–2c). The peaks at 612 cm^{-1} is assigned to the ZnS band (i.e., corresponding to sulphides). The samples heated at 700 and 900°C, show the band at 796 cm^{-1} (figure 2d and figure 2e) which is assigned to the ZnO band [8]. The band at 3469 cm^{-1} corresponds to valence vibrations of the occluded water. Our measurement of the spectrum of powdered sample yields the bands, which are in good agreement with the reported values. The changes in the observed values are due to the formation of nano phase. The bands around 483, 473 and 436 cm^{-1} are assigned to the Mn-O band at 700 and 900°C. Actually, at 900°C vibration level splits into 483 cm^{-1} and 436 cm^{-1} [9]. IR absorption peaks around 2300 cm^{-1} have completely disappeared at 900°C. Bands around 3000–3600 cm^{-1} are due to the hydrogen stretching frequency (OH stretching). Bands around 900–1500 cm^{-1} are due to the oxygen stretching and bending frequency. The additional weak bands and shoulders at 2921, 2847, 2353, 1634 and 1409 cm^{-1} may be due to the micro structural formation of the sample. Bands around 1200 and 1100 $cm^{\cdot -1}$ are due to the characteristic frequency of inorganic ions. Weak additional bands were observed at 992, 984 and 865 $cm^{\cdot -1}$ at lower temperature. These modes indicate the presence of resonance interaction between vibrational modes of sulphide ions in the crystal [9].

3.3 *EDAX study*

Figure 3 reveals that the Mn^{2+} ions may be incorporated in the Zn^{2+} lattice sites. We get the composition of our sample. About 60% of Zn^{+} ion and about 3% Mn ion by mass are present in the sample.

3.4 *Optical studies*

From figure 4, it can be seen that the strongest absorption peak of the as-prepared sample appears at around 300 nm, which is fairly blue-shifted from the absorption edge of the bulk ZnS (345 nm). ZnS has good absorption for light in the wavelength of 220–350 nm [10]. Semiconductor crystallites in the diameter range of a few nanometers show a three dimensional quantum size effect in their electronic

structure. These quantum size effects on the band gap absorption energy can be measured by UV-VIS absorption spectroscopy.

From the UV study we can calculate the energy band gap. Manifacier model is used to determine the absorption coefficient α from the transmittance data [11]. The fundamental absorption, which corresponds to the transmission from valence band to the conduction band, is employed to determine the band gap of the material.

From figure 5, we calculate the absorption coefficient (α). The relation between absorption coefficient (α) and incident photon energy ($h\nu$) can be written as

$$\alpha = A(h\nu - E_{\mathrm{g}})^n/h\nu,$$

where A is a constant and E_{g} is the band gap of the material.

Exponent n depends on the type of the transition, n may have values 1/2, 2, 3/2 and 3 corresponding to the allowed direct, allowed indirect, forbidden direct and forbidden indirect transitions respectively [12].

But in the nanocrystalline sample, there may be some deviation from the bulk like transition. From the above equation, it is clear that, plot of $(\alpha h\nu)^2$ vs. $h\nu$ will indicate a divergence at an energy value, E_{g} where the transition takes place. Taking the values at discontinuities as the band gap, the nature of the transition (i.e., the n value) is determined.

The exact value of the band gap is determined by extrapolating the straight line portion of $(\alpha h\nu)^2$ vs. $h\nu$ graph to the $h\nu$ axis. It was noticed that the band gap value is higher than the bulk value of ZnS. Table 4 gives the values of the band gap at different temperatures. The value is found to decrease and remains constant at higher temperatures which is due to the quantum confinement of the value [13]. Bhargava *et al* [14] suggested that with decreasing particle size a strong hybridization of the s-p states of the ZnS host and the d states of the Mn^{2+} impurity should occur. This hybridization results in a faster energy transfer between the ZnS host and Mn^{2+} impurity yielding a higher quantum efficiency and it was argued that through this hybridization, the spin-forbidden $^4T_1 - ^6A_1$ transition of the Mn^{2+} impurity becomes less spin-forbidden, resulting in a shorter decay time [5,15].

4. Conclusion

We have prepared Mn^{2+}-doped ZnS nanoparticles by chemical co-precipitation method. The structure, optical properties, band gap and composition of the samples were determined by XRD, FTIR, UV-VIS and EDAX spectra analyses. XRD analysis shows the sample prepared is in a hexagonal phase. The particle size can be adjusted by controlling the reaction temperature. Prominent IR peaks are analyzed and assigned. The strongest absorption peak appears at around 300 nm, which is fairly blue-shifted from the absorption edge of the bulk (345 nm). The solid-state theory based on the delocalized electron and hole within the confined volume can explain the blue-shifted optical absorption spectra. Band gap values were determined from the optical transmission studies of the as-prepared samples. The composition of the prepared sample is established from the EDAX on the sample. With decreasing particle size, a strong hybridization of the s-p states of the ZnS host and the d states of the Mn^{2+} impurity is likely to occur.

References

[1] D J Norris and M G Bawendi, *Phys. Rev.* **B53**, 16338 (1996)
[2] L W Wang and A Zunger, *J. Phys. Chem.* **B102**, 6449 (1998)
[3] Ye Changhui, Fang Xiaosheng, Li Guanghai and Zhang Lide, *Appl. Phys. Lett.* **85**, 15, 3035 (2004)
[4] H C Warad, S C Ghosh, B Hemtanon, C Thanachayanont and J Dutta, *Science Technol. Adv. Mater.* **6**, 296 (2005)
[5] O A Korotchenkov, A Cantarero, A P Shpak, Yu A Kunitskii, A I Senkevich, M O Borovoy and A B Nadtochii, *Nanotechnology* **16**, 2033 (2005)
[6] M Abdul Khader and Binny Thomas, *Nano structured materials* **10**, 4, 593 (1998)
[7] W Q Peng, G W Cong, S C Qu and Z G Wang, *Nanotechnology* **16**, 1469 (2005)
[8] Nakamota Kazuo, 5th ed. *Infrared and Raman spectra of inorganic and co-ordination compounds* (1972)
[9] Sibi Kurian, Shajo Sebastian, Jose Mathew and K C George, *Indian J. Pure Appl. Phys.* **42**, 926 (2004)
[10] Chen Jianfeng, Li Yaling, Wang Yuhong, Yun Jimmy and Cao Dapeng, *Mater. Res. Bull.* **39**, 185 (2004)
[11] Manifaqcier, M De Murcia, J P Fillard and E Vicario, *Thin Solid Films* **41**, 127 (1997)
[12] J I Pankove, *Optical processes in semiconductors* (Prentice-Hall, New Jersey, 1971)
[13] R Maity, S Kundoo, P K Ghosh and K K Chattopadhayay, *Indian J. Phys.* **A78(1)**, 121 (2004)
[14] R N Bhargava and D Gallagher, *Phys. Rev. Lett.* **72**, 416 (1994)
[15] A A Bol and A Meijerink, *J. Lumin.* **87–89**, 315 (2000)